Simulations and experiments of EMFY-1 electromagnetic launcher

Simulations and Experiments of EMFY-1 Electromagnetic Launcher

Doğa Ceylan, Mustafa Karagöz, Yasin Çevik, Baran Yıldırım, Hakan Polat, and Ozan Keysan

***Abstract*— ASELSAN Inc. has been conducting experimental research on electromagnetic launch technologies since 2014. The first prototype, EMFY-1, has 25 mm × 25 mm square bore and 3-m-length rails. In addition, two capacitor-based pulsed-power supplies (PPSs) with 1- and 4-MJ stored energy are built to supply launcher. During the design process of EMFY-1, a 3-D finite element (FE) model has been developed to simulate the electromagnetic and mechanical aspects of the railgun. This paper presents the simulation and experimental results of EMFY-1 with C-type aluminum armature. FE model, developed using COMSOL Multiphysics, includes both launcher and the PPS system. In addition to the velocity and position of the armature with respect to time, it is possible to observe the magnetic field, current density distributions and breech voltage using the FE model. In the experiments, pulse currents of the PPS modules, breech, and muzzle voltages are measured. The velocity of the projectile is measured using the B-dot probes. In this paper, two experiments of EMFY-1 will be presented. In the first experiment, the launch package with 42-g total mass is accelerated to 2778 m/s, and in the second experiment, the launch package with 130-g total mass is accelerated to 1560 m/s. The simulation results of the proposed FE model are compared with the experiments. It is observed that there is a good agreement between experimental and simulation results.**

***Index Terms*— Electromagnetic launch, finite element (FE) analysis, pulsed-power supply (PPS), railgun.**

I. Introduction

ELECTROMAGNETIC launcher is an accelerator concept which converts the electrical energy to kinetic energy. It basically consists of two conducting parallel rails, an armature, and a nonconducting projectile. A large amount of pulse-shaped current generated by a pulsed-power supply (PPS) flows through rails and armature in a short duration of time. Due to the Lorentz force acting on the armature, armature, and projectile accelerate between the rails.

Fair [1] discusses various concepts for the electromagnetic launch technology: armature types, rail/armature interface, pulsed-power generation, computational, and experimental tools. Unlike the traditional electrical machines, the operation time of electromagnetic launchers are a few milliseconds, the currents are in the order of hundreds of kiloamperes, the magnetic field densities in the launcher can exceed 20 T, and the exit velocity can be larger than 2000 m/s, which are not achievable with conventional gun-powder-based projectiles [2]. Therefore, critical design of rails and projectiles are necessary not only to be able to withstand high Lorentz forces and resistive losses, as explained in [3] and [4], but also to maximize the muzzle kinetic energy. In the design process of an electromagnetic launcher, besides the skin and the proximity effect, which are commonly taken into consideration in high-frequency fields, a phenomena called velocity skin effect (VSE) plays a significant role in the distribution of the current density in the rails, armature, and contact zone between them, as explained in [5]. Therefore, detailed finite element (FE) modeling of these effects is required in the investigation of these elements.

A 3-D FE model has been developed which is capable of simulating the launch process including both PPS and launcher. The first prototype called EMFY-1 is manufactured and tested using this simulation model. EMFY-1 was tested with different energy levels of the designed PPS and a C-shaped solid armature. In this paper, the details of EMFY-1 and the FE model will be explained. Moreover, the outputs of the FE model and the results of the experiments of EMFY-1 will be compared in order to verify the developed simulation model.

II. Properties of Electromagnetic Launcher System

EMFY-1 is the first electromagnetic launcher developed by ASELSAN Inc. (based in Ankara, Turkey) [6]. In 2016, a launch package with a total mass of 38 g was accelerated using EMFY-1 with 1-MJ PPS as a proof of concept [7], [8]. The muzzle velocity was found to be 1000 m/s. The results of these experiments were presented in [9]. After the first experiment, ASELSAN started developing a new capacitor-based PPS in order to increase the muzzle velocity and the mass of the launch package. For this goal, the total stored energy capacity of the PPS is increased to 4 MJ. However, during the experiments, EMFY-1 is tested with 850- and 992-kJ stored electrical energy.

A. Launcher

EMFY-1 is a 3-m, 25-mm square bore launcher. The cross section view of its rails is presented in Fig. 1, where w is

Manuscript received November 29, 2018; revised February 15, 2019 and March 15, 2019; accepted April 20, 2019. Date of publication May 31, 2019; date of current version July 9, 2019. This work was supported by ASELSAN Inc. The review of this paper was arranged by Senior Editor F. Hegeler.*(Corresponding author: Ozan Keysan.)*

D. Ceylan, H. Polat, and O. Keysan are with the Department of Electrical and Electronics Engineering, Middle East Technical University (METU), Ankara 06800, Turkey (e-mail: keysan@metu.edu.tr).

M. Karagöz, Y. Çevik, and B. Yıldırım are with ASELSAN Inc., Ankara 06370, Turkey (e-mail: mkaragoz@aselsan.com.tr).

Color versions of one or more of the figures in this paper are available online at http://ieeexplore.ieee.org.

Digital Object Identifier 10.1109/TPS.2019.2916220

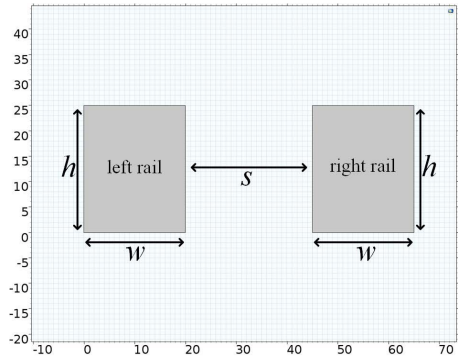

Fig. 1. Rail and rail separation dimensions on the rail cross section view.

TABLE I
GEOMETRIC PARAMETERS OF THE LAUNCHER

rail thickness: *w*	20 mm
rail height: *h*	25 mm
rail separation: *s*	25 mm
rail length: *l*	3 m

Fig. 2. EMFY-1 electromagnetic launcher.

the thickness of the rails, h is the height of the rails, and s is the rail separation. The values of these parameters are given in Table I.

EMFY-1 consists of a glass-reinforced composite body, copper alloy rail, and steel bolts that holds the housing intact. The mechanical structure of EMFY-1 electromagnetic launcher is presented in Fig. 2. Properties of the aluminum alloy used in the armature, copper alloy used in the rails, and steel alloy used in the containment are given in Table II. In the table, σ is the electrical conductivity, ρ is the density, and C_p is the heat capacity.

B. Pulsed Power Supply

A capacitor-based PPS topology is used to supply the launcher. The schematic of the short circuited (without launcher) single PPS module is given in [9]. The single

TABLE II
PROPERTIES OF ARMATURE, RAILS, AND CONTAINMENT MATERIALS

	σ (MS/m)	ρ (kg/m^3)	C_p (J/(kg*K))
Armature	19.2	2700	900
Rails	43.5	8960	385
Containment	1.74	7700	480

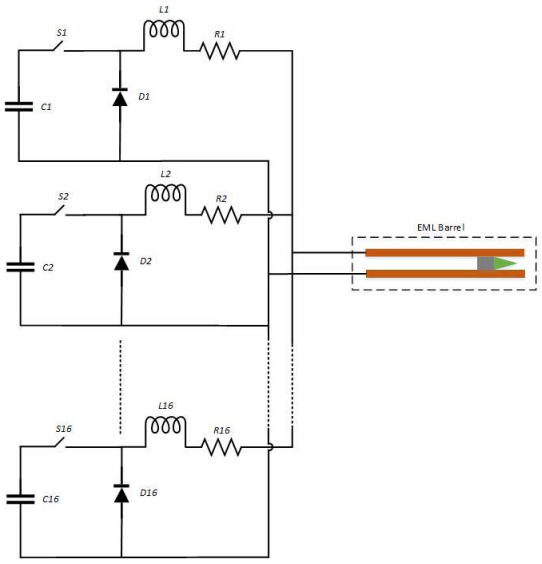

Fig. 3. Sixteen parallel connected modules supply the launcher.

Fig. 4. 4-MJ PPS of EMFY-1.

module of the designed PPS has 250-kJ stored electrical energy in this paper. The PPS of EMFY-1 contains 16 parallel connected modules, as shown in Fig. 3, each of which has 250-kJ initial energy, resulting in a total energy of 4 MJ.

The 4-MJ PPS is composed of a pulsed-power module container, a capacitor charger, and a control container. The pulsed-power module container contains 16 PPS modules and a control cabinet as shown in Fig. 4.

III. SIMULATION MODEL

Although developing a realistic FE model is critical for the design process of an electromagnetic launcher, it is also a challenging task. Wang *et al.* [10] explain the challenges of modeling the launch process in transient with a moving

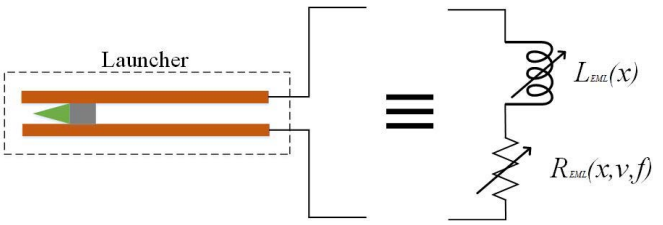

Fig. 5. Electromagnetic launcher can be modeled as series connected variable resistance and inductance.

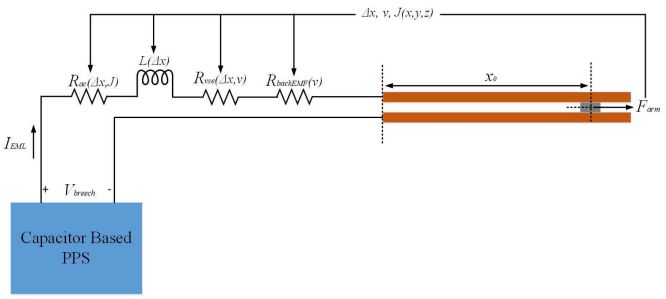

Fig. 6. Schematic of the FE model.

armature. Since the rail current has a pulse-shaped form, the magnetic field gradient becomes very large which makes the simulation problem difficult. Due to the large magnetic field gradient, the size of the mesh elements between the rails has to be fine enough for the computation of the Lorentz force acting on the armature. However, the length of the rails is much larger than the size of the mesh elements around them which increases the total number of elements and increases the computation time exponentially.

In addition, Lou *et al.* [11] investigate the circuit equation of an electromagnetic launcher. From the electrical point of view, a launcher can be represented as series-connected variable resistance and inductance as in Fig. 5. Although the inductance of the launcher depends on the position of the armature, its resistance depends on the position and velocity of the armature and also the frequency of the pulse-shaped supply current (as the current density distribution in the rails is not homogeneous due to the ac skin effect).

For large armature velocities, a current clustering occurs at the sliding contact interface that causes a huge current concentration near the trailing edge of the armature, which is also referred to as the VSE, as discussed in [5] and [12]. Therefore, it is not accurate to calculate the current waveform in the rails using a model with the stationary armature, as it ignores the influence of VSE phenomenon as stated in [13]. The contribution of VSE on the launcher resistance increases as the armature speed increases. On the one hand, it is not possible to build a realistic FE model without the VSE concept. On the other hand, an FE model with moving armature has large computational cost. In this paper, a new methodology is proposed that models the armature VSE by introducing series connected variable resistances and inductance to the electric equivalent circuit as shown in Fig. 6. In Fig. 6, I_{EML} is the rail current, V_{breech} is the breech voltage, F_{arm} is the electromagnetic force acting on the armature in the direction of acceleration, x_0 is the preload position (i.e., initial armature position), Δx is the displacement of the armature after the excitation, v is the velocity of the armature, $J(x, y, z)$ is the current density vectors inside the rails, $L(\Delta x)$ is the external inductance value of the launcher, $R_{\mathrm{ac}}(\Delta x, J)$ is the ac resistance of the launcher, $R_{\mathrm{vse}}(\Delta x, v)$ is the VSE resistance, and $R_{\mathrm{back\ EMF}}(v)$ is the resistance which represents the back EMF.

The proposed FE model includes both PPS and EMFY-1 launcher. Initial values of the external electrical parameters are set to zero. During the launch simulation, the armature velocity, displacement and the current density distribution are calculated in each time step to update the values of the external resistances and inductances. As it can be observed from Fig. 6, (1) and (2) can be written for the external parameters. The calculation of these external parameters will be discussed in the following sections

$$R_{\mathrm{EML}} = R_{\mathrm{ac}}(J, \Delta x) + R_{\mathrm{vse}}(\Delta x, v) + R_{\mathrm{back\ EMF}}(v) \quad (1)$$

$$L_{\mathrm{EML}} = L(\Delta x). \quad (2)$$

A. Calculation of Launcher Inductance ($L(\Delta x)$)

Keshtkar *et al.* [14] investigate the calculation of the inductance gradient of an electromagnetic launcher. Inductance gradient of an electromagnetic launcher is defined as the inductance value of the rails where the position of the armature is equal to 1 m. Also, it can be calculated using (3), where L' is the inductance gradient, F is the electromagnetic force acting on the armature in the armature acceleration direction, and I is the total supply current

$$L' = 2(F/I^2). \quad (3)$$

Since the inductance value of an electromagnetic launcher is linearly proportional to the armature position, the inductance value can be calculated as in (4), where x_0 is the preload position of the armature, Δx is the displacement of the armature after the excitation

$$L = (x_0 + \Delta x)L' = 2(x_0 + \Delta x)(F/I^2). \quad (4)$$

In (4), it is assumed that the total energy stored in the launcher inductance is equal to the work done by the electromagnetic force on the armature. However, this equation neglects the magnetic flux density distribution inside the rails, which affects the overall inductance calculation. In the proposed FE model, the definition of the inductance is used as in (5), where λ is the total magnetic flux, N is the number of turns, which is unity for this case, and ϕ is the magnetic flux. Therefore, the launcher inductance can be calculated more accurately as in (6) by integrating flux density distribution over the symmetry plane. In (6), $B_z(x, y)$ is the magnetic field in the z-direction and A is the integration area. Also, in Fig. 7, the integration area and z-direction used in (6) are shown. Since the direction of the magnetic field on that area can be in the $-z$-direction, negative magnetic field components are eliminated using the term $(B_z(x, y) > 0)$ in (6)

$$L = \frac{\lambda}{I} = \frac{N\phi}{I} = \frac{\phi}{I} \quad (5)$$

$$L = \frac{1}{I}\int_A \big(B_z(x, y) > 0\big) * B_z(x, y)dA. \quad (6)$$

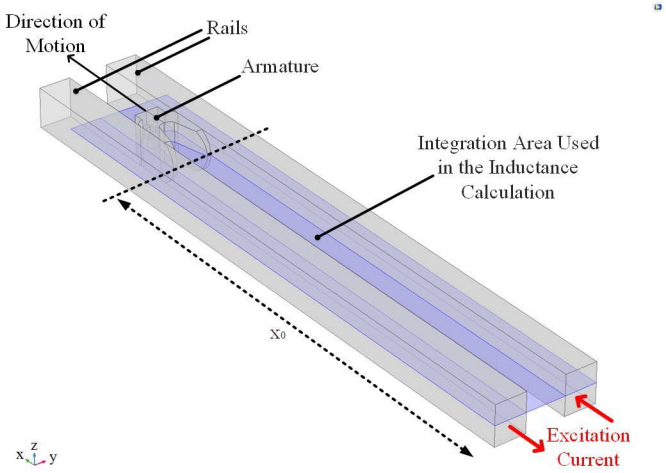

Fig. 7. Integration area used to calculate the inductance of the launcher.

B. Calculation of AC Resistance $(R_{\mathrm{ac}}(J, \Delta x))$

There are two electromagnetic phenomena that influence the current density distribution inside the rails: the skin effect and the proximity effect [15]. Since the excitation current is in pulse-shaped form, the magnitude of the current density near the rail surfaces is larger compared to the current density magnitude in the center of the cross section of the rails due to the skin effect. Also, current density concentrates on the facing (inner) surfaces of the rails due to the proximity effect. These two effects increase the rail resistance, especially during the current rising time interval. Since the analytic calculation of ac resistance is complex, using the FE method (FEM) for this purpose is reasonable. The developed FE model calculates the current density distribution in the rails and the external ac resistance used in the stationary FE model is calculated as in (7), where J is the current density, V is the rail volume, and ρ_{rail} is the resistivity of the rail material. The ac resistance is updated at each time step of the simulation. It should be noted that this approach neglects the current concentration on the contact surface. However, for large armature velocities, VSE is the dominant term on the contact transition as presented in [12]

$$R_{\mathrm{ac}} = \Delta x \frac{1}{I^2} \oint_{\mathrm{rail}} \left(\rho_{\mathrm{rail}} \left(\sqrt{J_x^2 + J_y^2 + J_z^2} \right)^2 \right) dV. \quad (7)$$

C. Calculation of Back EMF $(R_{\mathrm{BackEMF}}(v))$

The calculation of the launcher inductance voltage of an electromagnetic launcher is different from the calculation of an ordinary inductor voltage due to armature position and speed variation as presented in (8). Once the differentiation chain rule is applied, an extra term appears in the inductance voltage equation as in (9)

$$E = -\left[I(t) \frac{dL(x(t))}{dx} \frac{dx(t)}{dt} + L(x(t)) \frac{dI(t)}{dt} \right] \quad (8)$$

$$E = -\left[I(t)\, L'\, v(t) + L(x(t)) \frac{dI(t)}{dt} \right]. \quad (9)$$

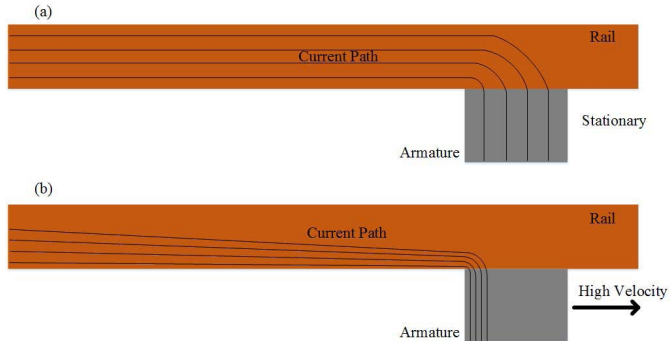

Fig. 8. Effect of VSE on the current path inside the rail, armature and contact zone.

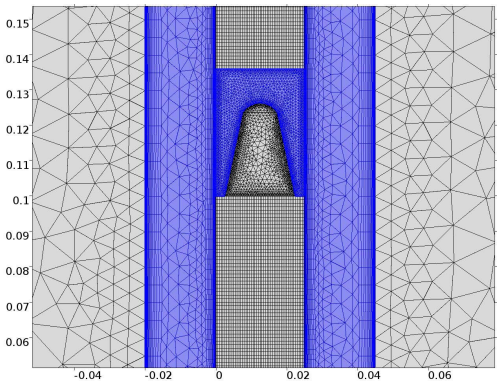

Fig. 9. Mesh design of the 2-D FE model with moving armature.

As the armature is assumed to be stationary in the proposed model, this extra term is included in the model as an external velocity-dependent resistance, called the back EMF resistance, as in (10). Although there is no physical meaning of the back EMF resistance like a resistive heat loss, it is required to include it to make the stationary model more accurate

$$R_{\mathrm{back\,emf}}(v(t)) = L'\, v(t). \quad (10)$$

D. Calculation of Velocity Skin Effect Resistance $(R_{vse}(\Delta x, v))$

Hsieh *et al.* [16] define the VSE as a current-clustering phenomenon caused by the high speed of the armature. VSE has a large influence on the current density distribution in the rails and armature. Therefore, it also effects the launcher resistance. A basic representation of the effect of VSE on the current density distribution is presented in Fig. 8.

Although, in [12], the equation for the VSE resistance is found as in (11), where K_{vse} is the VSE coefficient, the calculation of K_{vse} is not obtained analytically, but it is found experimentally with a collector test-rig experiment as presented in [17]

$$R_{\mathrm{vse}} = K_{\mathrm{vse}} v^{3/2}. \quad (11)$$

In order to find the relation between R_{vse} and the armature velocity, a 2-D FE model with moving armature is developed, the mesh design of which is shown in Fig. 9. In the developed

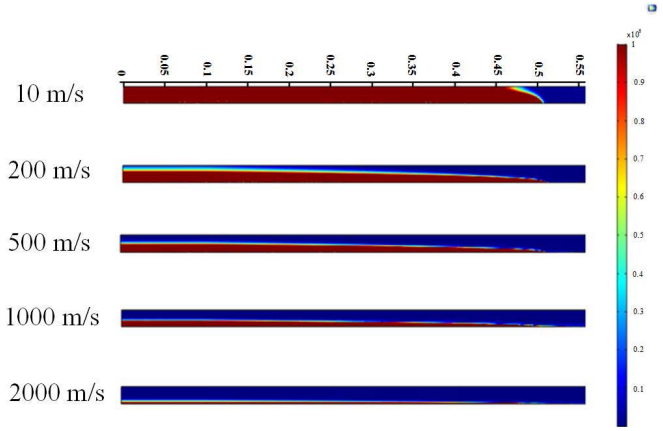

Fig. 10. Current density distributions in the rail for different armature velocities.

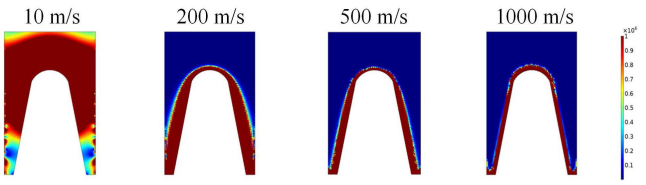

Fig. 11. Current density distributions in the armature for different armature velocities.

2-D FE model, the armature is moved with different constant velocities, and the variation of the current density distribution in the rails and armature is observed under dc excitation. Figs. 10 and 11 show the current density distribution at various speeds. From the figures, it can be observed that the effective area that conducts the current gets smaller as the velocity increases.

The VSE resistance of the rails and armature are calculated for different armature velocities using the current density distribution in the rails and armature as in the following equation, where h is the height of the rails, I is the dc rail current, ρ is the resistivity, J is the current density, and A is the area of rails and armature in the 2-D FE model:

$$R_{\text{vse}} = h\frac{1}{I^2}\int \left(\rho\left(\sqrt{J_x^2 + J_y^2 + J_z^2}\right)^2\right) dA. \tag{12}$$

Since the excitation current does not have any ac component, the calculated resistance values for different armature velocities are equal to R_{vse}. R_{vse} values are interpolated with respect to the armature velocity to be used in the 3-D FE model which is used for the simulation of EMFY-1.

IV. Experimental and Simulation Results

The open area launch tests of EMFY-1 were conducted in May 2018. In total, 52 experiments between 500- and 1500-kJ initial electrical energy had been conducted with various armature shapes. The analytical model is verified on all these experiments, however, only two of the experiments are presented. Also, the simulation results, calculated using the proposed FE code, will be discussed.

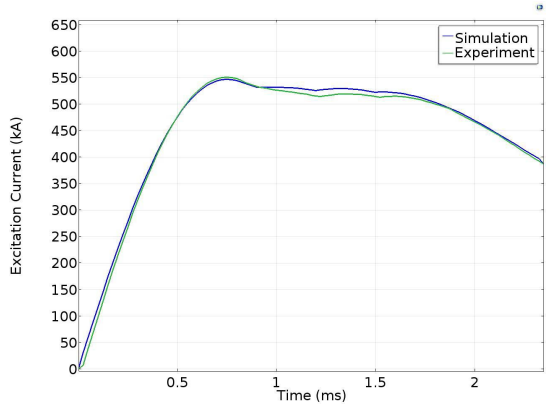

Fig. 12. Simulation and experimental results for the rail current of the experiment-A.

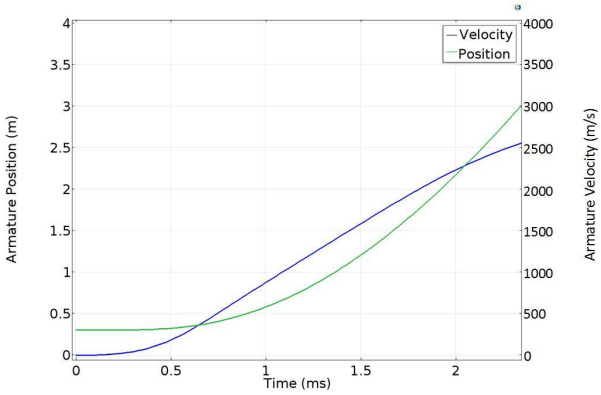

Fig. 13. Simulation results for the variation of armature position and velocity for the experiment-A.

A. Experiment-A (850 kJ, 42 g)

The total stored electrical energy of the PPS is adjusted to 850 kJ for this test. The mass of the launch package is chosen as 42 g.

The rail current waveform is shown in Fig. 12. The current waveform is given until 2.34 ms, which is the instant when the armature exits the rails. The peak value of the excitation current is calculated and measured as 550 kA. Fig. 12 shows the comparison between the experimental results and the developed FE model, which are in good agreement.

Simulation results for the armature velocity and position are shown in Fig. 13. The muzzle velocity is found to be 2590 m/s using the FE model. B-dot probe sensors are used to measure the launch package velocity inside the launcher. Furthermore, a high-speed camera system is used to measure the velocity after the armature leaves the launcher. The muzzle velocity is measured as 2778 m/s using these velocity measurement sensors.

The variation of the launcher resistance components, defined as external variable resistances in the simulation model, is shown in Fig. 14. It can be observed that the voltage drop due to the VSE resistance and back EMF becomes larger than the voltage drop due to the ac resistance after 0.7 ms. Therefore, it can be concluded that for higher velocities

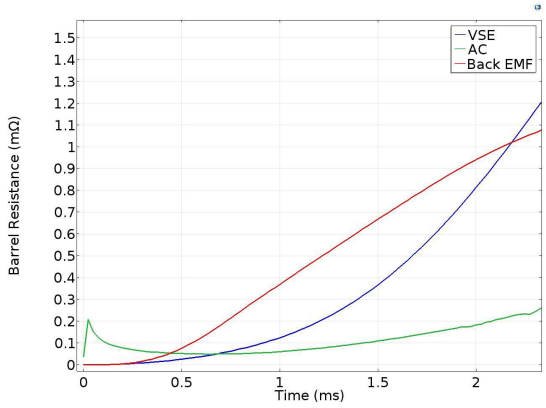

Fig. 14. Simulation results for the launcher resistance components of the experiment-A.

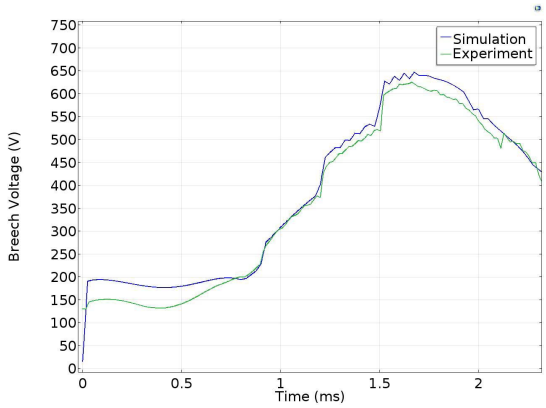

Fig. 15. Simulation and experimental results for the breech voltage of the experiment-A.

than 500 m/s, VSE resistance becomes the dominant parameter in the launcher resistance.

The breech voltage can be calculated using (13) in the simulation model. It is also measured during the experiments. The breech voltage waveforms simulated using the FE model and measured in the experiments are compared in Fig. 15. It can be observed that the maximum breech voltage is found to be approximately 650 V from both the simulation and experimental results

$$V_{\text{breech}} = R_{\text{ac}} I + R_{\text{back EMF}} I + R_{\text{vse}} I + L\frac{dI}{dt}. \qquad (13)$$

Although it is not possible to measure the magnetic flux density distribution around the armature during the launch, it is possible to observe it using the developed FE model. Normalized magnetic flux density distribution around the armature at 0.75 ms is shown in Fig. 16. It is observed that the maximum magnetic flux density behind the armature is calculated as 22.5 T. In addition, the average magnetic flux density between the rails is found to be 10 T.

A few important outcomes of the experiment and simulations are presented in Table III.

B. Experiment-B (992 kJ, 130 g)

Increasing the total mass, as well as increasing the muzzle velocity is the goal of the experiments with EMFY-1.

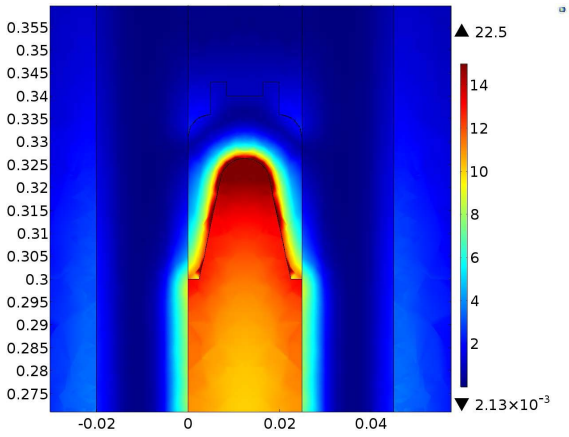

Fig. 16. Simulation result for the normalized magnetic flux density distribution of the experiment-A at 0.75 ms.

TABLE III
CRITICAL MEASUREMENTS FROM THE EXPERIMENT-A

Initial Electrical Energy	850 kJ
Launch Package Mass	42 g
Peak Rail Current	550 kA
Maximum Magnetic Flux Density	22.5 T
Armature Exit Time	2.34 ms
Muzzle Current	360 kA
Maximum Breech Voltage	650 V
Inductance Gradient	0.42 uH/m
Maximum Acceleration	152 10^3 g
Simulated Muzzle Velocity	2582 m/s
Experimental Muzzle Velocity	2778 m/s
Experimental Muzzle Kinetic Energy	162 kJ
Efficiency of the Total System	19%

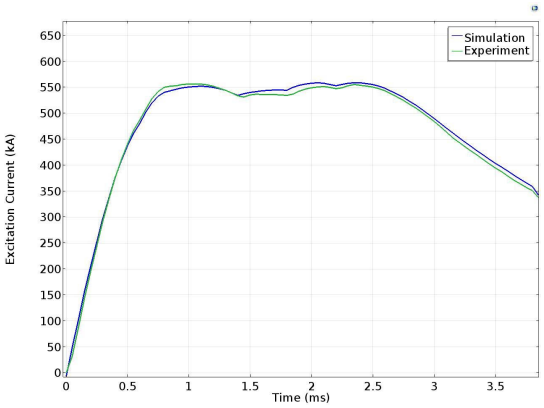

Fig. 17. Simulation and experimental results for the rail current of the experiment-B.

In experiment-B, the total mass of the launch package is increased to 130 g by adding a nonconducting mass in front of the conducting armature used in the experiment-A. The total stored electrical energy of the PPS is adjusted to 992 kJ. The waveform of the rail currents, calculated using the simulation model and measured in the experiment, are compared in Fig. 17. There exists a good agreement between them.

The launch package leaves the launcher at 3.84 ms after firing. The variation of the position and velocity of the launch

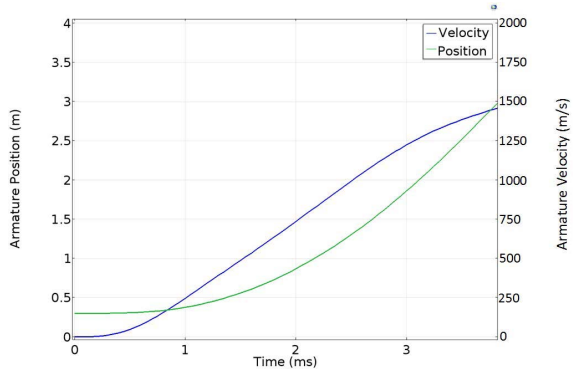

Fig. 18. Simulation results for the variation of armature position and velocity for the experiment-B.

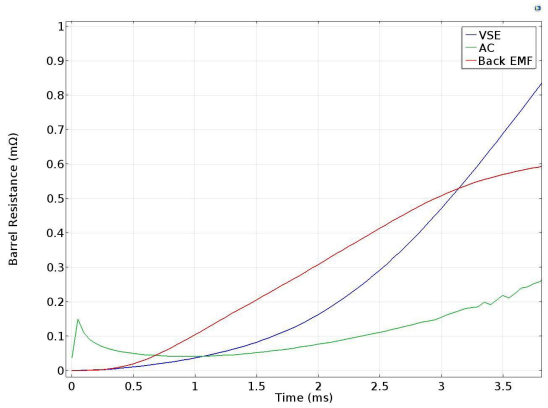

Fig. 19. Simulation results for the launcher resistance components of the experiment-B.

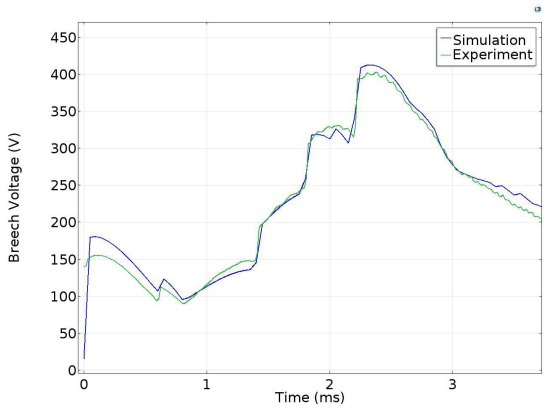

Fig. 20. Simulation and experimental results for the breech voltage of the experiment-B.

package, calculated from the FE model, is shown in Fig. 18. Although the muzzle velocity is calculated as 1480 m/s from the simulation, it is measured as 1560 m/s using the velocity measurement sensors.

The variation of the ac and VSE resistances are shown in Fig. 19. As observed in the Experiment-A, VSE resistance becomes larger than the ac resistance for the velocities larger than 500 m/s. In addition to ac and VSE resistances, the back EMF resistance which represents the voltage drop due to the change of the launcher inductance is also shown in Fig. 19.

TABLE IV
SOME CRITICAL OUTPUTS OF THE EXPERIMENT-B

Initial Electrical Energy	992 kJ
Mass of the Launch Package	130 g
Peak of the Rail Current	560 kA
Maximum Magnetic Flux Density	29.4 T
Armature Exit Time	3.84 ms
Muzzle Current	345 kA
Maximum Breech Voltage	410 V
Inductance Gradient	0.42 uH/m
Maximum Acceleration	53 10^3 g
Simulated Muzzle Velocity	1480 m/s
Experimental Muzzle Velocity	1560 m/s
Experimental Muzzle Kinetic Energy	158 kJ
Efficiency of the Total System	16%

This component also has a large influence on the breech voltage since it is dependent of armature velocity as shown in (10).

The result for the breech voltage, found from both simulations and the experiment, is compared in Fig. 20. From (13), it can be observed that the peak value of the breech voltage is highly dependent on the launch package velocity. Since the velocity in the Experiment-B is smaller than the one in the Experiment-A, the peak value of the breech voltage is found to be 410 V for the Experiment-B, which is smaller than the one in the Experiment-B. Significant parameters of the second experiment are given in Table IV to summarize the experiment.

V. CONCLUSION

ASELSAN Inc. has developed and tested its first electromagnetic launcher (EMFY-1) with 25 × 25 mm square bore and 3-m-length rails using C-type solid aluminum armature powered by 4-MJ capacitor-based PPS. An FE model is developed to analyze EMFY-1 launcher. The developed 3-D FE model, including both the PPS and the launcher, is able to simulate the effects of a moving armature with a stationary model using external variable resistances and inductance. This new approach decreases the computational cost significantly. The proposed FE model was verified with the experimental results. In the experiment-A, 42 g of launch package is accelerated to 2778 m/s with 850 kJ PPS. In the experiment-B, a 130 g launch package is launched with 992 kJ PPS. The muzzle velocity is measured as 1560 m/s. The efficiencies are measured as 19% and 16%, respectively. In addition to the given velocity and position data, the proposed launcher resistance components show that for velocities higher than 500 m/s, the velocity dependent resistances, which are VSE and back EMF resistances, become larger than the ac resistance.

ACKNOWLEDGMENT

The authors would like to thank the A. Civil, B. Yurdakul, E. Durna, E. Tan, Ö. Cavbozar, U. Göçmen, and U. Türeli of the ASELSAN Team, whose support made this paper possible.

REFERENCES

[1] H. D. Fair, "Advances in electromagnetic launch science and technology and its applications," *IEEE Trans. Magn.*, vol. 45, no. 1, pp. 225–230, Jan. 2009.

[2] S. Hundertmark, M. Schneider, and G. Vincent, "Payload acceleration using a 10-MJ DES railgun," *IEEE Trans. Plasma Sci.*, vol. 41, no. 5, pp. 1455–1459, May 2013.

[3] T. G. Engel, M. J. Veracka, and J. M. Neri, "The specific-force performance parameter for electromagnetic launchers," *IEEE Trans. Plasma Sci.*, vol. 38, no. 2, pp. 194–198, Feb. 2010.
[4] M. Ghassemi and R. Pasandeh, "Thermal and electromagnetic analysis of an electromagnetic launcher," *IEEE Trans. Magn.*, vol. 39, no. 3, pp. 1819–1822, May 2003.
[5] Q.-A. Lv *et al.*, "Physical principle and relevant restraining methods about velocity skin effect," *IEEE Trans. Plasma Sci.*, vol. 43, no. 5, pp. 1523–1530, May 2015.
[6] ASELSAN Inc. *ASELSAN Official Website*. Accessed: Nov. 29, 2018. [Online]. Available: http://www.aselsan.com.tr/en-us/Pages/default.aspx
[7] M. Karagöz, O. Cavbozar, A. Civil, Y. Çevik, E. Tan, and E. Durna, "Design and testing of a 1 MJ pulsed power supply," in *Proc. 18th EML Symp.*, Wuhan, China, 2016.
[8] Y. Çevik, E. Durna, and M. Karagöz, "Design and experimental validation of complete block diagram model for a pulsed power supply," in *Proc. 18th EML Symp.*, Wuhan, China, 2016.
[9] M. Karagoz *et al.*, "ASELSAN EMFY-1 electromagnetic launcher: First experiments," in *Proc. IEEE 21st Int. Conf. Pulsed Power*, Jun. 2017, pp. 1–3.
[10] G.-H. Wang, L. Xie, Y. He, S.-Y. Song, and J.-J. Gao, "Moving mesh FE/BE hybrid simulation of electromagnetic field evolution for railgun," *IEEE Trans. Plasma Sci.*, vol. 44, no. 8, pp. 1424–1428, Aug. 2016.
[11] Y. Lou, G. Wan, Y. Jin, B. Tang, and B. Li, "Research on energy loss distribution of an augmented railgun," *IEEE Trans. Plasma Sci.*, vol. 44, no. 5, pp. 857–861, May 2016.
[12] T. G. Engel, J. M. Neri, and M. J. Veracka, "Characterization of the velocity skin effect in the surface layer of a railgun sliding contact," *IEEE Trans. Magn.*, vol. 44, no. 7, pp. 1837–1844, Jul. 2008.
[13] T. Stankevič, M. Schneider, and S. Balevičius, "Magnetic diffusion inside the rails of an electromagnetic launcher: Experimental and numerical studies," *IEEE Trans. Plasma Sci.*, vol. 41, no. 10, pp. 2790–2795, Oct. 2013.
[14] A. Keshtkar, S. Mozaffari, and A. Keshtkar, "Inductance gradient variation with time and armature sliding along the rails," *IEEE Trans. Plasma Sci.*, vol. 39, no. 1, pp. 75–79, Jan. 2011.
[15] Z. Pang, H. Wang, H. Wang, and L. Zhang, "Analysis of current and magnetic field distributions in rail launcher with peaceman–rachford finite-difference method," *IEEE Trans. Plasma Sci.*, vol. 40, no. 10, pp. 2717–2722, Oct. 2012.
[16] K.-T. Hsieh, F. Stefani, and S. J. Levinson, "Numerical modeling of the velocity skin effects: An investigation of issues affecting accuracy," *IEEE Trans. Magn.*, vol. 37, no. 1, pp. 416–420, Jan. 2001.
[17] L. E. Thurmond, B. K. Ahrens, and J. P. Barber, "Measurement of the velocity skin effect," *IEEE Trans. Magn.*, vol. 27, no. 1, pp. 326–328, Jan. 1991.

Doğa Ceylan received the B.Sc. and M.Sc. degrees from the Department of Electrical and Electronics Engineering, Middle East Technical University (METU), Ankara, Turkey, in 2016 and 2018, respectively, where he is currently pursuing the Ph.D. degree.

He is currently a Researcher with METU. His current research interests include design and optimization of electrical machines, electric vehicles, electromagnetic launchers, pulsed-power sources, and renewable energy.

Mustafa Karagöz received the B.Sc. and M.Sc. degrees from the Department of Electrical and Electronics Engineering, Middle East Technical University (METU), Ankara, Turkey, in 2010 and 2014, respectively.

Since 2010, he has been with ASELSAN Inc., Ankara, where he has been a Technical Project Manager in an electromagnetic railgun project since 2014. His current research interests include electromagnetic launch and pulsed power technologies.

Yasin Çevik received the B.Sc. and M.Sc. degrees in electrical and electronics engineering from Middle East Technical University (METU), Ankara, Turkey, in 2011 and 2015, respectively.

He is currently an Electronics Design Research and Development Engineer with ASELSAN Inc., Ankara. His current research interests include electromagnetic launchers and pulsed-power sources.

Baran Yıldırım received the B.Sc. degree from the Department of Mechanical Engineering, Middle East Technical University (METU), Ankara, Turkey, in 2008, and the master's and Ph.D. degrees from Northeastern University, Boston, MA, USA, in 2010 and 2013, respectively.

He is currently an Analysis and Test Engineer with ASELSAN Inc., Ankara. His current research interests include specialty include solid mechanics, impact mechanics, finite element analysis, modeling of dynamic systems, kinematic, and dynamic measurement of structures.

Hakan Polat received the B.Sc. degree from the Department of Electrical and Electronics Engineering, Middle East Technical University (METU), Ankara, Turkey, in 2018, where he is currently pursuing the M.Sc. degree.

His current research interests include design and optimization of electrical machines, electromagnetic launchers, pulsed-power sources, power electronics, and renewable energy.

Ozan Keysan received the B.Sc. and M.Sc. degrees from Middle East Technical University (METU), Ankara, Turkey in 2005 and 2008, respectively, and the Ph.D. degree from the University of Edinburgh, Edinburgh, U.K., in 2014.

He is currently an Assistant Professor with the Department of Electrical and Electronics Engineering, METU. His current research interests include renewable energy, design and optimization of electrical machines, smart grids, superconducting machines, and permanent-magnet machines.